Regional neuroinflammation caused by peripheral infection is involved in fatigued symptoms: A [18F]DPA-714 PET study

Yuta Ochi
RIKEN Center for Biosystems Dynamics Research
Di Hu
RIKEN Center for Biosystems Dynamics Research
Danxi Li
RIKEN Center for Biosystems Dynamics Research
Wakiko Arakaki
RIKEN Center for Biosystems Dynamics Research
Aya Mawatari
RIKEN Center for Biosystems Dynamics Research
Mika Shigeta
RIKEN Center for Biosystems Dynamics Research
Yuping Wu
RIKEN Center for Biosystems Dynamics Research
Emi Hayashinaka
RIKEN Center for Biosystems Dynamics Research
Hiroyuki Neyama
RIKEN Center for Biosystems Dynamics Research
Tsuyoshi Tahara
RIKEN Center for Biosystems Dynamics Research
Yasuhiro Wada
RIKEN Center for Biosystems Dynamics Research
Feng Li
Beijing University of Chinese Medicine
Hisashi Doi
RIKEN Center for Biosystems Dynamics Research
Yasuyoshi Watanabe
RIKEN Center for Biosystems Dynamics Research
Yilong Cui (cuiyl@riken.jp)
RIKEN Center for Biosystems Dynamics Research

Research Article

Keywords: fatigue-like symptoms, regional neuroinflammation, peripheral infection, PET, sickness behavior

Posted Date: July 27th, 2022

DOI: https://doi.org/10.21203/rs.3.rs-1875953/v1

Abstract

A series of symptoms, including fever, widespread pain, fatigue, and even ageusia, have frequently been reported in the context of various infections, such as COVID-19. Although the pathogenic mechanisms underlying an infection causing fever and pain have been well established, the mechanisms of fatigue induced by infection remain unclear. To elucidate whether and how the peripheral infection cause fatigue via regional neuroinflammation, we performed a brain-wide investigation of neuroinflammation in a peripheral pseudoinfection rat model using [^{18}F]DPA-714 positron emission tomography (PET) imaging analysis, in which the polyriboinosinic: polyribocytidylic acid (poly I:C) was intraperitoneally injected. Consistent with previous reports, transient fever lasting for several hours and subsequent suppression of spontaneous activity lasting a few days were induced by poly I:C treatment. Significant increase in plasma interleukin (IL)-1β, IL-6 and tumour necrosis factor (TNF)-α were observed at 2 and 4 h following poly I:C treatment. PET imaging analysis revealed that the brain uptake of [^{18}F]DPA-714 was significantly increased in several brain regions one day after poly I:C treatment, such as the dorsal raphe (DR), parvicellular part of red nucleus (RPC), A5 and A7 noradrenergic nucleus, compared with the control group. The accumulation of [^{18}F]DPA-714 in the DR, RPC and A5 was positively correlated with the fatigue-like behavior, and that in the A7 tended to positively correlate with fever. These findings suggest that peripheral infection may trigger regional neuroinflammation, which may cause specific symptoms such as fatigue. A similar mechanism might be involved in COVID-19.

Introduction

Infections induced by various kinds of pathogens or pathogenic organisms are known to be associated with a series of symptoms including fever, widespread pain, and fatigue. The underlying mechanisms for infection-evoked fever have been well investigated. A lipid mediator, prostaglandin (PG) E2, is produced and increased in the brain parenchyma in response to peripheral infection, subsequently activating the EP3 receptors of thermoregulatory neurons in the preoptic area of the hypothalamus, leading to a fever [1, 2]. A growing body of investigation has also demonstrated that both the central and peripheral mechanisms are involved in infection-induced pain. For example, upregulation of the transient receptor potential family in the primary afferent sensory neurons in response to the pro-inflammatory mediator is known to be crucial to hyperalgesia [3, 4]. Long-term debilitating fatigue and severe fatigue sensations have also been reported frequently in various infections. In 1985, there was an outbreak of illness characterized by chronic or recurrent debilitating fatigue linked to the Epstein–Barr virus in Nevada in USA. The illness was defined as chronic fatigue syndrome (CFS) by the Centers for Disease Control and Prevention and first described in a publication in 1988 [5]. Thereafter, similar symptoms have been frequently reported in some virus infections, including coronavirus disease 2019 (COVID-19). The latest clinical studies in COVID-19 have mentioned that besides respiratory symptoms, fatigue is one of the most common (approximately 50%) typical clinical manifestations related to COVID-19, and might be observed as sequelae [6, 7, 8]. However, the detailed mechanisms pointing to the involvement of infection in fatigue pathophysiology remain unclear, and conclusive evidence has yet to be demonstrated.

Recently, neuroinflammation has been proposed as a possible mechanism related to the development of fatigue. Neuroinflammation, an immune response in the central nervous system (CNS) whereby glial cells are activated, is known to be involved in a variety of CNS diseases, not only neurodegenerative diseases but also neuropsychiatric disorders. In a pioneering study, Nakatomi *et al.*[9] reported that widespread neuroinflammation, particularly in the hippocampus, amygdala, thalamus, and midbrain, was observed in patients with CFS. Besides, neuroinflammation in patients with the Gulf war syndrome with a similar phenotype to CFS was observed in the precuneus, prefrontal, primary motor and somatosensory cortices [10]. Although peripheral infection has been reported to trigger inflammatory responses in the brain [11, 12, 13], the underlying mechanisms for fatigue involved in neuroinflammation in the specific brain regions remain unclear.

The regional neuroinflammation in the brain could be quantitatively evaluated by positron emission tomography (PET) imaging non-invasively using radiolabeled compounds targeting specific biomarkers of activated glial cells. A mitochondrial outer membrane protein, translocator protein 18 kD (TSPO), has been widely used as a reliable biomarker for neuroinflammation due to its unique expression pattern, it is rarely expressed in the resting microglia but is drastically upregulated in the activated microglia [14]. The pyrazolopyrimidine compound DPA-714 has a higher affinity for TSPO and has been labeled with fluorine-18 by Kassiou's group as a second generation specific radioligand for TSPO [15]. [^{18}F]DPA-714 has been demonstrated to have better brain uptake and improved signal-to-noise ratio than [^{11}C]PK11195, the gold standard PET probe for TSPO, and has been widely used for the quantitative assessment of neuroinflammation in CNS diseases, including stroke [16], trauma [17], epileptic seizures [18], Alzheimer's disease [19], and amyotrophic lateral sclerosis [20]. To investigate whether and how the regional neuroinflammation is involved in peripheral infection induced fatigue-like symptoms, we induced a peripheral pseudoinfection in rats by intraperitoneal injection of polyriboinosinic: polyribocytidylic acid (poly I:C), a synthetic double-stranded RNA which has been widely used to mimic peripheral viral infections [21]. Using this animal model, we performed brain-wide quantitative evaluation of neuroinflammation using [^{18}F]DPA-714 PET imaging analysis and assessed the correlation between regional neuroinflammation and sickness behaviors, including fatigue.

Materials And Methods

Animals and peripheral pseudoinfection generation

Forty-six male Sprague-Dawley rats (6 weeks old) were purchased from Japan SLC (Hamamatsu, Japan). The rats were housed in a temperature- (23 ± 1°C), humidity- (60 ± 5%), and light- (lights on at 8:00 and off at 20:00) controlled environment. A standard laboratory diet and tap water were available *ad libitum*. For acclimation, rats were housed in the experimental room for at least 1 week before the week-long pre-level measurement of spontaneous activity, and randomly divided into saline- (control) and poly I:C-treated groups. A pseudo-viral infection in rats (8 weeks old) was induced by intraperitoneal injection of poly I:C (GE Healthcare Life Science, Buckinghamshire, UK), a synthetic double-stranded RNA, dissolved in saline at a dose of 10 mg/kg body weight [21, 22]. In the control

group, rats were injected with saline at analogous procedure. The injection was performed between 10:00 and 11:00 in the morning. The experimental procedures in the present study were approved by the Institutional Animal Care and Use Committee of RIKEN, Kobe Branch, and were performed in accordance with the *Guide for the care and use of laboratory animals* (NIH publication No. 85-23, revised 2011).

Measurement of spontaneous activity

To quantitatively evaluate fatigue state, the spontaneous activity of each rat was recorded with an infrared beam sensor (NS-AS01; Neuroscience Inc., Tokyo, Japan) prior to and following a poly I:C injection. The infrared beam sensor was placed 15 cm above the center of each cage, and the activities of rats housed in individual cages were measured. The level of night-time spontaneous activity was normalized by the mean value of the 3 days prior to poly I:C injection. The fatigue of rats was calculated by assessing night-time spontaneous activity, which was added up every 60 min and analyzed in Clock Lab (Neuroscience Inc.). In addition, the spontaneous activity in all rats used in [^{18}F]DPA-714 PET scan was also examined separately throughout the entire experimental period for the correlation analysis.

Body temperature measurement

Body temperature of rats was monitored using an implantable programmable temperature transponder (IPTT-300, Bio Medic Data Systems, Inc., Seaford, USA), which was implanted gently into the subcutaneous tissue between the scapulae of each rat under anesthesia (with a mixture of 1.5% isoflurane and nitrous oxide/oxygen 7:3) with a syringe-like action 7 days before intraperitoneal injection of poly I:C or saline. Temporal changes in the body temperature of the rats were measured wirelessly using an IPTT reader from 0 h (before injection) to 48 h following the poly I:C or saline injection.

Cytokine analysis

Besides the pre-injection levels, at 2 h, 4 h, 8 h, 24 h, and 48 h after poly I:C injection, rats were shortly anesthetized with a mixture of 1.5% isoflurane and nitrous oxide/oxygen (7:3), and blood samples were collected from an indwelling catheter in the tail vein implanted prior to sampling. Venous blood was centrifuged at 12,000 rpm for 10 min at 4°C and cytokine levels were measured on the resulting plasma. The cytokines IL-1β, IL-6 and TNF-α were simultaneously assessed using the Bio-Plex Pro Rat Cytokines Assay (Bio-Rad Laboratories Inc., California, USA) according to the manufacturer's instructions [23].

PET scanning

In the present study, [^{18}F]DPA-714 was synthesized as reported by Sydney group [24]. The product was identified and purified using high-performance liquid chromatography on a COSMOSIL C18-AR-II column (10 × 250 mm, Nacalai, Kyoto, Japan). Molar activity ranged from 33 to 160 GBq/μmol. Radiochemical purity analyzed using HPLC exceeded 99%.

All PET scans were performed using a microPET Focus220 (Siemens, Knoxville, USA) designed for small laboratory animals. Rats were anesthetized with 1.5% isoflurane and nitrous oxide/oxygen (7:3) and placed in a prone position in the PET scanner gantry. During the PET scan, the body temperature was maintained at 37°C using a small animal warmer connected to a thermometer (BWT-100A; Bio Research Center, Nagoya, Japan). A 45-min emission scan was performed immediately after the bolus injection of [^{18}F]DPA-714 (≈75 MBq per animal) via a cannula inserted into the tail vein; the energy window was 400–650 keV and the coincidence time window was 6 ns. Emission data were collected in list mode and sorted into dynamic sonograms (6 × 10 s, 6 × 30 s, 11 × 60 s, and 10 × 180 s, for a total of 33 frames). The acquired data were reconstructed by standard 2D-filtered back projection (FBP) (ramp filter, cutoff frequency at 0.5 cycles per pixel) for quantification, and by a statistical maximum a posteriori probability (MAP) algorithm (12 iterations with point spread function effect) for image registration.

Image analysis

PET images were co-registered to a magnetic resonance imaging (MRI) template which was placed in a Paxinos and Watson stereotactic space using the PMOD imaging processing software (version 3.6, PMOD Technologies, Ltd, Zürich, Switzerland). Each FBP image was spatially smoothed using an isotropic Gaussian kernel (0.6-mm FWHM) for enhancement of the statistical power. The radioactivity was normalized with cylinder phantom data and expressed as standardized uptake values (SUVs).

A voxel-based statistical analysis was performed using SPM 8 software (Welcome Department of Imaging Neuroscience, London, UK). A two sample *t*-test was used for estimating the statistical differences between groups. The statistical threshold was set to be $P < 0.005$ (FWE) with an extent threshold of 200 contiguous voxels.

Statistical analysis

All results are expressed as the mean ± SEM. All data were analyzed in SPSS (version 24.0, IBM, Armonk, USA). A one-way analysis of variance (ANOVA) with Bonferroni's multiple-comparison procedure was used to assess changes in body temperature, cytokines, and spontaneous activity prior to and following the poly I:C injection. A two-way repeated measures ANOVA with a Bonferroni's multiple-comparison procedure was used to assess differences in body temperature and spontaneous activity between the two groups of rats. A Pearson's test was used for correlation analysis of accumulation of [^{18}F]DPA-714 in each brain region and fatigue-like behavior. Differences were considered statistically significant for $P < 0.05$.

Data availability

The data that support the findings of this study are available on request from the corresponding author.

Results

Poly I:C-induced symptoms and plasma cytokine elevation

Poly I:C has been widely used to induce sickness behaviors, such as fever, pain, and fatigue, as well as body weight loss [21]. As expected, the body weight of poly I:C-treated rats decreased approximately by 10% of the pre-level value the day after poly I:C injection, thereafter recovering gradually. To assess poly I:C-induced fever, subcutaneous body temperature was measured in a free-moving condition with a wireless temperature transponder from both the saline- and poly I:C-treated groups. As shown in Fig 1A, body temperature increased significantly in both groups within the first hour following intraperitoneal injection, as an acute stress response of the handling. Thereafter, the body temperature of rats in the poly I:C-treated group increased significantly again and reached a peak at 5 h after the poly I:C injection (one-way repeated measures ANOVA, $P < 0.001$). In addition, it was significantly higher than that in the control group from 2 to 7 h after the intraperitoneal injection (two-way repeated measures ANOVA, $P < 0.001$).

To assess poly I:C-induced peripheral inflammatory responses, temporal changes in plasma cytokines were detected up to 48 h after the poly I:C injection (Fig 1B). Several pro-inflammatory cytokines were significantly elevated at early injection time points, as compared with the pre-level. Two hours after poly I:C injection, cytokines IL-1β (one-way ANOVA, $P < 0.001$; Bonferroni's $P = 0.019$), IL-6 (one-way ANOVA, $P < 0.001$; Bonferroni's $P = 0.004$) and TNF-α (one-way ANOVA, $P < 0.001$; Bonferroni's $P < 0.001$) were significantly elevated. A significant elevation of IL-1β (Bonferroni's $P = 0.002$) and IL-6 (Bonferroni's $P = 0.006$) was observed until 4 h following the poly I:C injection.

Poly I:C-induced suppression of spontaneous activity

Fatigue can be assessed by changes in voluntary activity, known to be associated with motivation [21]. To evaluate fatigue, night-time spontaneous activity in the home cage was investigated in both groups. As shown in Fig 2, the night-time spontaneous activity in the control group remained nearly stable throughout the experiment. However, the night-time spontaneous activity decreased significantly on the first night after the poly I:C injection (post day 1, one-way ANOVA, $P < 0.001$; Bonferroni's $P < 0.001$). On the second night (post day 2), the night-time spontaneous activity sharply recovered to 78 ± 4% (Bonferroni's $P < 0.001$) of its pre-level, and gradually returned to baseline level within 1 week. A significant difference in night-time spontaneous activity between the two groups was observed until day 5 post-injection (two-way repeated measures ANOVA, $P < 0.001$).

Peripheral infection-induced neuroinflammation

In order to confirm whether the peripheral infection would induce neuroinflammation in the brain, a PET scan with [^{18}F]DPA-714 was performed in rats from both groups 1 day after the poly I:C or saline injection. As shown in the representative PET images (Fig 3), [^{18}F]DPA-714 radioactivity was barely observed within the brain in the saline-injected rats, except in the choroid plexus in the cerebral ventricles and some surrounding circumventricular area. However, the radioactivity of [^{18}F]DPA-714 apparently increased throughout the brain regions after the poly I:C injection, especially in the mesencephalon and medulla, as well as in the cerebellum. Subsequently, a brain-wide statistical analysis was used to identify

brain regions in which accumulation of [^{18}F]DPA-714 increased significantly by the peripheral infection. A voxel-based statistical analysis showed that the accumulation of [^{18}F]DPA-714 significantly increased in the several brain regions following poly I:C injection, including the dorsal raphe (DR), parvicellular part of red nucleus (RPC), central medial thalamic nucleus (CM), parabrachial nucleus (PB), gigantocellular reticular nucleus (Gi), A5, A7, A11 nuclei, and so on (Fig 4 and Table 1).

Finally, to assess whether and how those regional neuroinflammations cause peripheral infection-induced symptoms, we analyzed the correlation between the [^{18}F]DPA-714 accumulation in all the brain regions showing significant increment and the fever or fatigue-like behavior. The correlation analysis revealed that the [^{18}F]DPA-714 accumulation in the DR, RPC and A5 positively correlated with the persistent fatigue severity defined by decrease in spontaneous activity from day 2 to day 5 following the poly I:C injection (Fig 5A to C). Moreover, a tendency towards a positive correlation of the [^{18}F]DPA-714 accumulation with body temperature was observed in the A7 noradrenergic nucleus (Fig 5D).

Discussion

In this study, we demonstrated that regional neuroinflammation caused by peripheral infection could be involved in fatigue and related symptoms, such as fever. Here, we provide lines of evidence that 1) transient fever and suppressed spontaneous activity lasting a few days were observed after an intraperitoneal injection of poly I:C, which has been widely used for induction of pseudoinfection; 2) an increased accumulation of [^{18}F]DPA-714 was found in widespread brain regions 1 day after treatment with poly I:C; 3) a voxel-based statistical analysis showed that a significant increment of [^{18}F]DPA-714 accumulation in the brain regions was closely related to fatigue-like behavior. Indeed, the accumulation of [^{18}F]DPA-714 in the DR, RPC, and A5, was positively correlated with fatigue severity, and that in the A7 tended to positively correlate with fever. To our knowledge, this is the first brain-wide investigation to determine the region specific neuroinflammation induced by peripheral infection that may relate to fatigue and specific related symptoms.

Peripheral infection is thought to trigger neuroinflammation via several mechanisms including neural and humoral signalling pathways. The involvement of afferent nerves, such as the vagal or trigeminal nerves, has been proposed in that the sustained activation of the primary afferent nerve terminal stimulated by an inflammatory mediator, such as IL-1β, sensitizes innervating structures and may initiate immune response in the surrounding brain parenchyma [25]. Consistently, we found that the accumulation of [^{18}F]DPA-714 in the afferent area of the vagal nerve was significantly increased, including in the bilateral nucleus tractus solitarius and parabrachial nucleus (Fig. 4), indicating that peripheral poly I:C treatment-induced neuroinflammation is thought to be mediated by the vagal afferent nerve in this experiment. Another plausible pathway consists of pro-inflammatory cytokines and their receptors in endothelial cells. In the present study, we found that plasma concentrations of several cytokines, including IL-1β, IL-6, and TNF-α, were increased and remained as such for hours after poly I:C treatment, as reported previously [26, 27]. Circulating IL-1β is known to activate the IL-1 receptors present on perivascular macrophages and

endothelial cells, resulting in an increase in prostaglandin E2 synthesis in the brain parenchyma [28, 29]. These two signalling pathways mentioned above might represent the pathways for conveying immune signals from the periphery to the brain in this study.

The main finding of the present study is that regional neuroinflammation in several brain regions may relate to the pathophysiology of fatigue-like symptoms following peripheral infection, such as the DR, RPC, and A5. Since a PET imaging technique provides a non-invasive approach for the quantitative evaluation of neuroinflammation *in vivo*, the association of regional neuroinflammation with consequent behavioral changes may be observed in the same animal. In the present study, we found that the peripheral infection-induced regional neuroinflammation in the DR was positively correlated with the subsequent fatigue-like symptoms. The DR is the largest serotonergic nucleus sending abundant projection fibers into widespread areas of the forebrain. Functional alternations in the brain serotonergic system have long been implicated in fatigue development and sensation [30]. In exercise-induced acute/physiological fatigue, the increased biosynthesis and release of serotonin (5-HT) in several brain regions have been reported to be involved in fatigue sensations [31, 32]. In contrast, selective serotonin reuptake inhibitors, which result in an increase in extracellular serotonin concentration, have been demonstrated to be effective for some patients with CFS. A gene polymorphism analysis in CFS patients by our group demonstrated that the frequency of longer (L or XL) allelic variants of the 5-HT transporter (5-HTT) promoter region was significantly increased compared to that in controls, pointing to elevated 5-HTT expression and low levels of extracellular 5-HT concentrations in CFS patients [33]. Moreover, clinical studies have also demonstrated that the upregulation of 5-HTT and consequent reduction of extracellular 5-HT levels were observed in IFN-α and IFN-γ therapies to treat various forms of cancer and hepatitis C, in which patients often complain of serious tiredness [34, 35]. In the case of CFS, we found a decrease in 5-HTT in the anterior cingulate cortex in the patients as compared with age- and sex-matched healthy controls [36], suggesting that the presynaptic components of afferent nerve from DR in the anterior cingulate cortex might be reduced in CFS patients with 5-hydroxy-*L*-[^{11}C]tryptophan and PET (unpublished data by Watanabe *et al.*). These observations suggest that the dysfunction of serotonergic system could represent an underlying mechanism involved at least in chronic/pathogenic fatigue. Taken together with the fact that neuroinflammation is known to induce dysfunction of or decline in regional neural activity [37, 38], these results in the present study suggest that regional neuroinflammation in the DR probably cause fatigue-like behavior via functional changes in the serotonergic system. In addition, neuroinflammation in the RPC and the A5 noradrenergic nucleus were also positively associated with fatigue-like behavior. Recently, a positive correlation has been reported between the magnitude of atrophy in the superior cerebellar peduncle (Scp) which envelops and traverses the RPC at all rostrocaudal leves, and fatigue severity in multiple sclerosis patients [39], and such volumetric variation in the Scp was then considered as an early structural change preceding fatigue development [40]. Overall, these observations suggest that regional neuroinflammation in these brain areas could be a plausible mechanism underlying peripheral infection-induced fatigue-like symptoms. Incidentally, chronic fatigue has been reported to be one of most frequently reported symptoms following COVID-19 infection [7, 8], suggesting that a similar

mechanism underlying neuroinflammation in multiple brain regions might be involved in such fatigue evoked by COVID-19.

In the present study, we also found that neuroinflammation in several other brain regions, including the A7, A11, CM, PB, and Gi, was significantly increased, but was not correlated with fatigue-like behavior. The tendency towards a positive association between [^{18}F]DPA-714 accumulation in the A7 and fever was observed following poly I:C treatment. The A7 noradrenergic nucleus has been reported to send inhibitory innervation to the sympathetic thermoregulation nucleus and the rostral medullary raphe (RMR), which facilitates tail artery vasoconstriction and brown adipose tissue thermogenesis, resulting in heat production and a reduction in heat loss [41]. Consistently, Nakamura *et al.*[1, 42] have demonstrated that the inhibitory EP3 PGE2 receptor is expressed in the A7 noradrenergic nucleus, suggesting that peripheral infection-induced PGE2 in the A7 suppresses the inhibitory innervation of A7 noradrenergic nucleus to the RMR, resulting in fever following poly I:C treatment. The weak correlation between regional neuroinflammation in the A7 and fever might be derived from the miss-matched [^{18}F]DPA-714 PET scan timing. In the present study, the [^{18}F]DPA-714 PET scans was performed 24 hours after poly I:C injection, whereas, the poly I: C injection-induced fever was peaked at 2 to 6 hours and recovered within 24 hours after treatment (Fig. 1A). Meanwhile, the regional neuroinflammation in the A7, A11, CM, PB, and Gi might be related to peripheral infection-induced pain since most of them have been reported to be involved in pain transmission and perception [43, 44, 45, 46, 47]. Taken together, these results suggested that the peripheral infection-induced diverse symptoms were probably attributed to regional neuroinflammation in specific brain areas.

Additionally, since the PB and nucleus tractus solitarius are well known to convey nucleus relay peripheral sensory input to higher order brain regions including the gustatory sensation [48], the present demonstration of regional neuroinflammation in the PB and nucleus tractus solitarius after the peripheral infection could be inferred as evidence of and a mechanism underlying the disturbances in taste due to viral infections, as was frequently reported in patients with COVID-19 in the clinic [49, 50].

Conclusions

In conclusion, in the present study, we performed a brain-wide investigation to provide conclusive evidence of the brain regions of peripheral infection-induced neuroinflammation. We also demonstrated the effect of regional neuroinflammation to fatigue and specific related symptoms. Future research is needed to further clarify the multiple interactions of these symptoms, which will aid in the development of more effective treatment strategies based on anti-inflammatory effects to address all fatigue related symptoms.

List Of Abbreviations

5-HT
5-hydroxy-tryptamine (serotonin)

5-HTT
5-HT transporter
CFS
Chronic fatigue syndrome
COVID-19
Novel coronavirus disease 2019
FBP
Filtered back projection
IL
Interleukin
PG
Prostaglandin
Poly I
C:Polyriboinosinic:polyribocytidylic acid
TNF-α
Tumour necrosis factor-α

Declarations

Funding

This work was supported in part by JSPS KAKENHI Grant Numbers JP17H02172 to Y.C. and 20K21777 to Y.C., and by AMED under Grant Numbers JP18dk0310068 to Y.W., JP20ak0101059 to Y.W. and Y.C., and JP20ak0101063 to Y.W. and Y.C.

Competing Interests

The authors have no competing interests to declare.

Author Contributions

Yuta Ochi, Di Hu, Danxi Li: Data acquisition, and interpretation writing and revising the manuscript

Wakiko Arakaki, Aya Mawatari: synthetic design and PET probe labeling

Mika Shigeta, Yuping Wu, Emi Hayashinaka: PET imaging acquisition, reconstruction and interpretation

Hiroyuki Neyama, Tsuyoshi Tahara: experimental design, and revising the manuscript

Yasuhiro Wada: PET imaging study design and interpretation

Hisashi Doi: PET probe synthetic design and interpretation, revising the manuscript

Feng Li, Yasuyoshi Watanabe: data interpretation and revising the manuscript

Yilong Cui: conception and design of study, interpreting data and revising the manuscript

Availability of data and materials

The datasets used and/or analyzed during the current study are available from the corresponding author on reasonable request.

Ethics approval

The experimental procedures in the present study were approved by the Institutional Animal Care and Use Committee of RIKEN, Kobe Branch, and were performed in accordance with the *Guide for the care and use of laboratory animals* (NIH publication No. 85-23, revised 2011).

Consent to participate

Not applicable.

Consent for publication

Not applicable.

Acknowledgement

We appreciate Masahiro Kurahashi of Sumitomo Heavy Industry Accelerator Service Ltd. for operation of the cyclotron.

References

1. Nakamura K, Matsumura K, Kaneko T, Kobayashi S, Katoh H, Negishi M. The Rostral Raphe Pallidus Nucleus Mediates Pyrogenic Transmission from the Preoptic Area. J Neurosci. 2002; 22:4600–4610.
2. Yamagata K, Matsumura K, Inoue W, Shiraki T, Suzuki K, Yasuda S, Sugiura H, Cao C, Watanabe Y, Kobayashi S. Coexpression of Microsomal-Type Prostaglandin E Synthase with Cyclooxygenase-2 in Brain Endothelial Cells of Rats during Endotoxin-Induced Fever. J Neurosci. 2001; 21:2669–2677.
3. Lapointe TK, Altier C. The role of TRPA1 in visceral inflammation and pain. Channels. 2011; 5:525–529.
4. Fernandes ES, Russell FA, Spina D, Mcdougall JJ, Graepel R, Gentry C, Staniland AA, Mountford DM, Keeble JE, Malcangio M, et al. A distinct role for transient receptor potential ankyrin 1, in addition to transient receptor potential vanilloid 1, in tumor necrosis factor α-induced inflammatory hyperalgesia and Freund's complete adjuvant-induced monarthritis. Arthritis Rheum. 2011; 63:819–829.
5. Holmes GP, Kaplan JE, Gantz NM, Komaroff AL, Schonberger LB, Straus SE, Jones JF, Dubois RE, Cunningham-Rundles C, Pahwa S. Chronic fatigue syndrome: a working case definition. Ann Intern Med. 1988; 108:387–389.

6. Yang J, Zheng Y, Gou X, Pu K, Chen Z, Guo Q, Ji R, Wang H, Wang Y, Zhou Y. Prevalence of comorbidities and its effects in patients infected with SARS-CoV-2: a systematic review and meta-analysis. Int J Infect Dis. 2020; 94:91–95.
7. Huang C, Wang Y, Li X, Ren L, Zhao J, Hu Y, Zhang L, Fan G, Xu J, Gu X, et al. Clinical features of patients infected with 2019 novel coronavirus in Wuhan, China. The Lancet. 2020; 395:497–506.
8. Qin C, Zhou L, Hu Z, Zhang S, Yang S, Tao Y, Xie C, Ma K, Shang K, Wang W, Tian DS. Dysregulation of Immune Response in Patients With Coronavirus 2019 (COVID-19) in Wuhan, China. Clin Infect Dis. 2020; 71:762–768.
9. Nakatomi Y, Mizuno K, Ishii A, Wada Y, Tanaka M, Tazawa S, Onoe K, Fukuda S, Kawabe J, Takahashi K, et al. Neuroinflammation in Patients with Chronic Fatigue Syndrome/Myalgic Encephalomyelitis: An ^{11}C-(R)-PK11195 PET Study. J Nucl Med. 2014; 55:945–950.
10. Alshelh Z, Albrecht DS, Bergan C, Akeju O, Clauw DJ, Conboy L, Edwards RR, Kim M, Lee YC, Protsenko E, et al. In-vivo imaging of neuroinflammation in veterans with Gulf War illness. Brain Behav Immun. 2020; 87:498–507.
11. von Zahn J, Möller J, Kettenmann H, Nolte C. Microglial phagocytosis is modulated by pro- and anti-inflammatory cytokines. Neuroreport. 1997; 8:3851–3856.
12. Dantzer R, Konsman JP, Bluthé RM, Kelley KW. Neural and humoral pathways of communication from the immune system to the brain: parallel or convergent? Auton Neurosci. 2000; 85:60–65.
13. Banks WA. The blood-brain barrier in neuroimmunology: Tales of separation and assimilation. Brain Behav Immun. 2015; 44:1–8.
14. Chen MK, Guilarte TR. Translocator protein 18 kDa (TSPO): Molecular sensor of brain injury and repair. Pharmacol Ther. 2008; 118:1–17.
15. Chauveau F, van Camp N, Dollé F, Kuhnast B, Hinnen F, Damont A, Boutin H, James M, Kassiou M, Tavitian B. Comparative Evaluation of the Translocator Protein Radioligands ^{11}C-DPA-713, ^{18}F-DPA-714, and ^{11}C-PK11195 in a Rat Model of Acute Neuroinflammation. J Nucl Med. 2009; 50:468–476.
16. Martín A, Boisgard R, Thézé B, van Camp N, Kuhnast B, Damont A, Kassiou M, Dollé F, Tavitian B. Evaluation of the PBR/TSPO Radioligand [18F]DPA-714 in a Rat Model of Focal Cerebral Ischemia. J Cereb Blood Flow Metab. 2010; 30:230–241.
17. Wang Y, Yue X, Kiesewetter DO, Niu G, Teng G, Chen X. PET imaging of neuroinflammation in a rat traumatic brain injury model with radiolabeled TSPO ligand DPA-714. Eur J Nucl Med Mol Imaging. 2014; 41:1440–1449.
18. Kaneko K, Irie S, Mawatari A, Igesaka A, Hu D, Nakaoka T, Hayashinaka E, Wada Y, Doi H, Watanabe Y, Cui Y. [^{18}F]DPA-714 PET imaging for the quantitative evaluation of early spatiotemporal changes of neuroinflammation in rat brain following status epilepticus. Eur J Nucl Med Mol Imaging. 2022; 49:2265–2275.
19. Keller T, Lopez-Picon FR, Krzyczmonik A, Forsback S, Kirjavainen AK, Takkinen JS, Alzghool O, Rajander J, Teperi S, Cacheux F, et al. [(18)F]F-DPA for the detection of activated microglia in a

mouse model of Alzheimer's disease. Nucl Med Biol. 2018; 67:1–9.

20. Corcia P, Tauber C, Vercoullie J, Arlicot N, Prunier C, Praline J, Nicolas G, Venel Y, Hommet C, Baulieu JL, et al. Molecular Imaging of Microglial Activation in Amyotrophic Lateral Sclerosis. PLoS ONE. 2012; 7:e52941.
21. Yamato M, Tamura Y, Eguchi A, Kume S, Miyashige Y, Nakano M, Watanabe Y, Kataoka Y. Brain Interleukin-1β and the Intrinsic Receptor Antagonist Control Peripheral Toll-Like Receptor 3-Mediated Suppression of Spontaneous Activity in Rats. PLoS ONE. 2014; 9:e90950.
22. Vasiadi M, Newman J, Theoharides TC. Isoflavones inhibit poly(I:C)-induced serum, brain, and skin inflammatory mediators - relevance to chronic fatigue syndrome. J Neuroinflammation. 2014; 11.
23. Feng Y, Chen L, Luo Q, Wu M, Chen Y, Shi X. Involvement of microRNA-146a in diabetic peripheral neuropathy through the regulation of inflammation. Drug Des Devel Ther. 2018; Volume 12:171–177.
24. James ML, Fulton RR, Vercoullie J, Henderson DJ, Garreau L, Chalon S, Dolle F, Selleri S, Guilloteau D, Kassiou M. DPA-714, a New Translocator Protein–Specific Ligand: Synthesis, Radiofluorination, and Pharmacologic Characterization. J Nucl Med. 2008; 49:814–822.
25. Maier SF, Goehler LE, Fleshner M, Watkins LR. The role of the vagus nerve in cytokine-to-brain communication. Ann N Y Acad Sci. 1998; 840:289–300.
26. Dilger RN, Johnson RW. Behavioral assessment of cognitive function using a translational neonatal piglet model. Brain Behav Immun. 2010; 24:1156–1165.
27. Seki C, Oh-Nishi A, Nagai Y, Minamimoto T, Obayashi S, Higuchi M, Takei M, Furutsuka K, Ito T, Zhang MR, et al. Evaluation of [11C]oseltamivir uptake into the brain during immune activation by systemic polyinosine-polycytidylic acid injection: a quantitative PET study using juvenile monkey models of viral infection. EJNMMI Res. 2014; 4.
28. Townsend BE, Johnson RW. Sulforaphane reduces lipopolysaccharide-induced proinflammatory markers in hippocampus and liver but does not improve sickness behavior. Nutr Neurosci. 2017; 20:195–202.
29. van Dam AM, de Vries HE, Kuiper J, Zijlstra FJ, De Boer AG, Tilders FJ, Berkenbosch F. Interleukin-1 receptors on rat brain endothelial cells: a role in neuroimmune interaction? FASEB J. 1996; 10:351–356.
30. Watanabe Y. PET/SPECT/MRI/fMRI Studies in the Myalgic Encephalomyelitis/Chronic Fatigue Syndrome. In PET and SPECT in Psychiatry. Edited by Dierckx RAJO, Otte A, de Vries EFJ, van Waarole A: Springer; 2021: 985–1001
31. Blomstrand E, Celsing F, Newsholme EA. Changes in plasma concentrations of aromatic and branched-chain amino acids during sustained exercise in man and their possible role in fatigue. Acta Physiol Scand. 1988; 133:115–121.
32. Davis JM, Alderson NL, Welsh RS. Serotonin and central nervous system fatigue: nutritional considerations. Am J Clin Nutr. 2000; 72:573S-578S.
33. Narita M, Nishigami N, Narita N, Yamaguti K, Okado N, Watanabe Y, Kuratsune H. Association between serotonin transporter gene polymorphism and chronic fatigue syndrome. Biochem Biophys

Res Commun. 2003; 311:264–266.

34. Capuron L. Neurobehavioral Effects of Interferon-α in Cancer Patients Phenomenology and Paroxetine Responsiveness of Symptom Dimensions. Neuropsychopharmacology. 2002; 26:643–652.
35. Wichers M, Maes M. The psychoneuroimmuno-pathophysiology of cytokine-induced depression in humans. Int J Neuropsychopharmacol. 2002; 5:375–388.
36. Yamamoto S, Ouchi Y, Onoe H, Yoshikawa E, Tsukada H, Takahashi H, Iwase M, Yamaguti K, Kuratsune H, Watanabe Y. Reduction of serotonin transporters of patients with chronic fatigue syndrome. Neuroreport. 2004; 15:2571–2574.
37. Saloner R, Cherner M, Grelotti DJ, Paolillo EW, Moore DJ, Heaton RK, Letendre SL, Kumar A, Grant I, Ellis RJ. Lower CSF homovanillic acid relates to higher burden of neuroinflammation and depression in people with HIV disease. Brain Behav Immun. 2020; 90:353–363.
38. Imran M, Al Kury LT, Nadeem H, Shah FA, Abbas M, Naz S, Khan AU, Li S. Benzimidazole Containing Acetamide Derivatives Attenuate Neuroinflammation and Oxidative Stress in Ethanol-Induced Neurodegeneration. Biomolecules. 2020; 10:108.
39. Bernitsas E, Yarraguntla K, Bao F, Sood R, Santiago-Martinez C, Govindan R, Khan O, Seraji-Bozorgzad N. Structural and Neuronal Integrity Measures of Fatigue Severity in Multiple Sclerosis. Brain Sci. 2017; 7:102.
40. Yarraguntla K, Seraji-Bozorgzad N, Lichtman-Mikol S, Razmjou S, Bao F, Sriwastava S, Santiago-Martinez C, Khan O, Bernitsas E. Multiple Sclerosis Fatigue: A Longitudinal Structural MRI and Diffusion Tensor Imaging Study. J Neuroimaging. 2018; 28:650–655.
41. Yoshida K, Li X, Cano G, Lazarus M, Saper CB. Parallel Preoptic Pathways for Thermoregulation. J Neurosci. 2009; 29:11954–11964.
42. Nakamura K, Li YQ, Kaneko T, Katoh H, Negishi M. Prostaglandin EP3 receptor protein in serotonin and catecholamine cell groups: a double immunofluorescence study in the rat brain. Neuroscience. 2001; 103:763–775.
43. Mravec B, Bodnar I, Uhereczky G, Kvetnansky R, Palkovits M. Effect of lesions of A5 or A7 noradrenergic cell group or surgical transection of brainstem catecholamine pathways on plasma catecholamine levels in rats injected subcutaneously by formalin. Gen Physiol Biophys. 2012; 31:247–254.
44. Liu S, Tang Y, Shu H, Tatum D, Bai Q, Crawford J, Xing Y, Lobo Mk, Bellinger L, Kramer P, Tao F. Dopamine receptor D2, but not D1, mediates descending dopaminergic pathway–produced analgesic effect in a trigeminal neuropathic pain mouse model. Pain. 2019; 160:334–344.
45. Sun Y, Wang J, Liang S, Ge J, Lu Y, Li J, Chen Y, Luo D, Li H, Li Y. Involvement of the Ventrolateral Periaqueductal Gray Matter-Central Medial Thalamic Nucleus-Basolateral Amygdala Pathway in Neuropathic Pain Regulation of Rats. Front Neuroanat. 2020; 14:32.
46. Roeder Z, Chen Q, Davis S, Carlson JD, Tupone D, Heinricher MM. Parabrachial complex links pain transmission to descending pain modulation. Pain. 2016; 157:2697–2708.

47. Nakamoto H, Soeda Y, Takami S, Minami M, Satoh M. Localization of calcitonin receptor mRNA in the mouse brain: coexistence with serotonin transporter mRNA. Brain Res Mol Brain Res. 2000; 76:93–102.
48. Chen JY, Campos CA, Jarvie BC, Palmiter RD. Parabrachial CGRP Neurons Establish and Sustain Aversive Taste Memories. Neuron. 2018; 100:891–899.e895.
49. Xydakis MS, Dehgani-Mobaraki P, Holbrook EH, Geisthoff UW, Bauer C, Hautefort C, Herman P, Manley GT, Lyon DM, Hopkins C. Smell and taste dysfunction in patients with COVID-19. Lancet Infect Dis. 2020; 20:1015–1016.
50. Mullol J, Alobid I, Mariño-Sánchez F, Izquierdo-Domínguez A, Marin C, Klimek L, Wang DY, Liu Z. The Loss of Smell and Taste in the COVID-19 Outbreak: a Tale of Many Countries. Curr Allergy Asthma Rep. 2020; 20.

Tables

Table 1

Brain regions of significantly increased [^{18}F]DPA-714 accumulation following peripheral pseudo infection

		T value	Volume
Brain regions	**Laterality**	**(peak)**	**(mm^3)**
Ventromedial thalamic nucleus, VM	R	9.88	0.16
A11 dopaminergic nucleus, A11	L/R	12.02/10.04	0.5/0.19
Red nucleus, parvicellular part, RPC	L	11.76	0.45
Medial geniculate nucleus, MG	R	11.46	1.39
Mesencephalic reticular formation, mRT	R	10.7	0.68
Dorsal raphe nucleus, DR		10.09	0.17
Dorsolateral periaqueductal gray, DLPAG	R	10.42	0.77
Hippocampus, HC	L	10.5	0.63
Precuneiform area, PrCnF	R	10.8	0.6
Subiculum, transition area, STr	R	10.9	0.37
Entothinal cortex, Ent	R	11.4	0.61
Parasubiculum, PaS	L	10.4	0.34
Cuneiform nucleus, CnF	R	11.31	0.58
Parabrachial nucleus, PB	L/R	12.37/11.4	0.74/0.36
A7 noradrenergic nucleus, A7	L/R	9.83/11.76	0.27/1.25
Pontine reticular nucleus, oral part, PnO	L	9.29	0.96
A5 noradrenergic nucleus, A5	R	12.46	0.98
Gigantocellular reticular nucleus, Gi	R	10.82	0.67
nucleus tractus solitarius, Sol	L/R	9.93/11.56	0.13/0.75
Inferior colliculus/Cerebellum, IC/Cb		13.34	29.58

Note: Vehicle (Saline) (n = 8) versus Poly I:C (10 mg/kg) (n = 8). Height threshold: T = 9.14 with an extent threshold of 200 contiguous voxels, $p < 0.005$ Familywise Error (FWE) corrected.

Figures

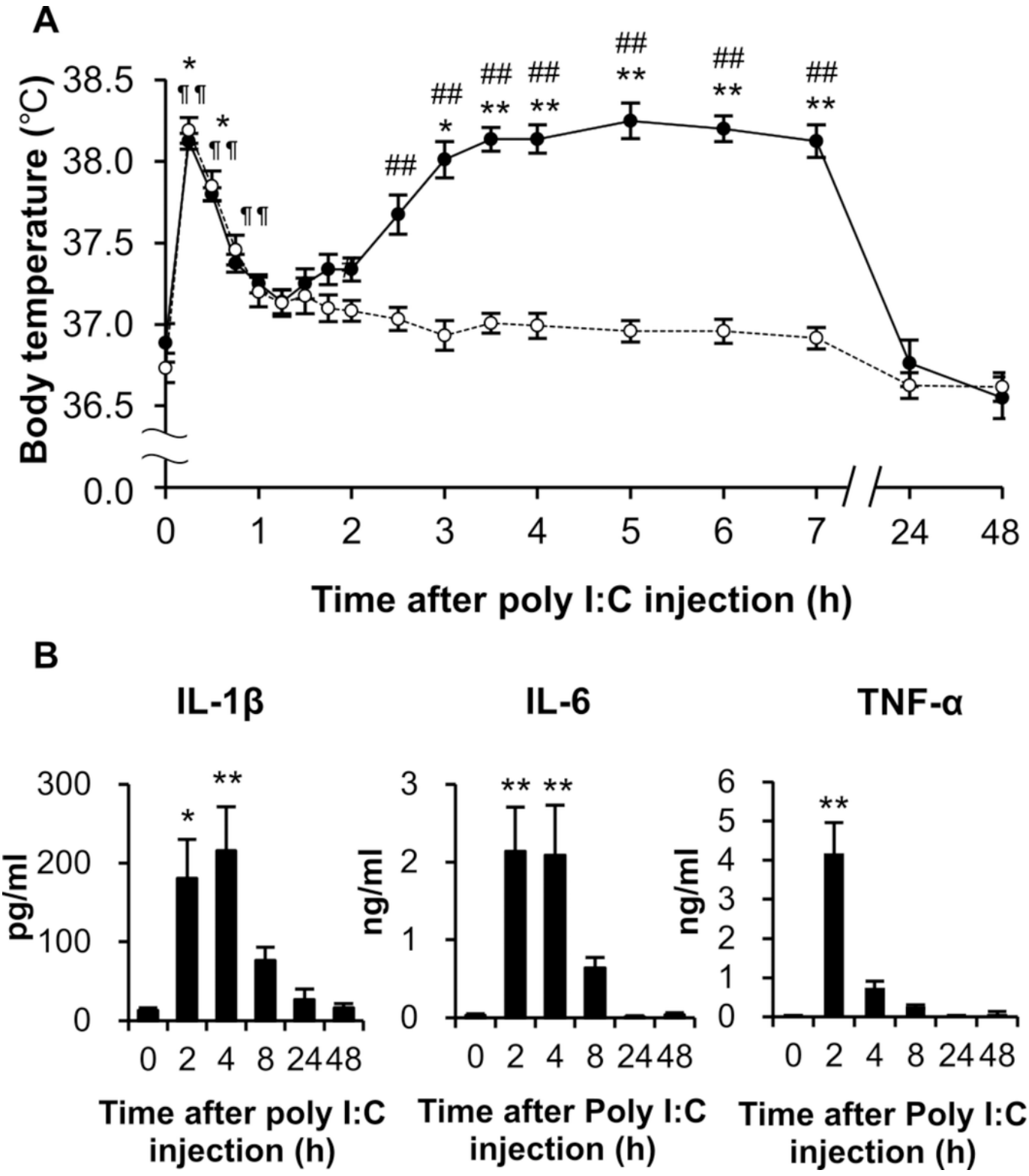

Figure 1

Temporal changes in body temperature and peripheral cytokines following an poly I:C or saline treatment.

(A) Subcutaneous body temperature of rats from poly I:C (10 mg/kg) treated group (closed circles, *n* = 8) and control group (open circles, *n* = 12) up to 48 h after intraperitoneal injection with poly I:C or saline were plotted. **P* < 0.05, ***P* < 0.01 for poly I:C-treated group, ¶¶ *P* < 0.01 for control group vs. 0 h (before

injection), one-way repeated measures ANOVA followed by Bonferroni's multiple-comparison procedure. $^{\#}P < 0.05$, $^{\#\#}P < 0.01$ vs. control group, two-way repeated measures ANOVA. **(B)** Plasma IL-1β, IL-6, and TNF-α were detected at 2 h, 4 h, 8 h, 24 h and 48 h following poly I:C injection, as well as pre-injection (0 h). Each value represents the mean ± SEM, $n = 14$. $^{*}P < 0.05$, $^{**}P < 0.01$ vs. pre-treated level, one-way ANOVA followed by Bonferroni's multiple-comparison procedure.

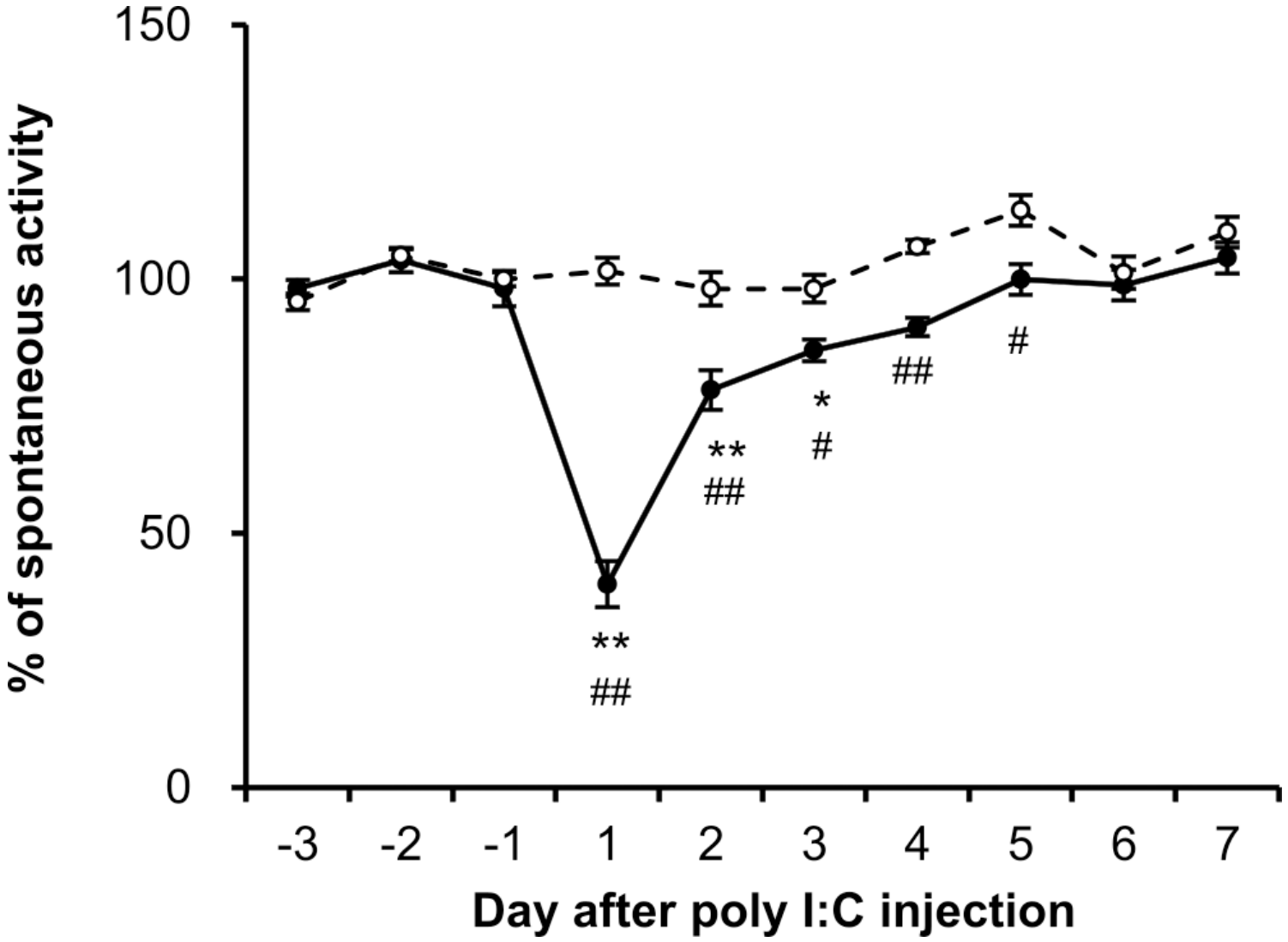

Figure 2

Dynamics of night-time spontaneous activity induced by poly I:C intraperitoneal injection.

The spontaneous activity of each rat from control (open circles, $n = 6$) and poly I:C-treated (closed circles, $n = 6$) groups was recorded from 3 days prior to injection, and the percentage of night-time spontaneous activity was normalized by the mean value over the course of the 3 days (-3 to -1). Each value represents the mean ± SEM. $^{*}P < 0.05$, $^{**}P < 0.01$ vs. pre-injection level, one-way ANOVA followed by Bonferroni's multiple-comparison procedure. $^{\#}P < 0.05$, $^{\#\#}P < 0.01$ vs. control group, two-way repeated measures ANOVA.

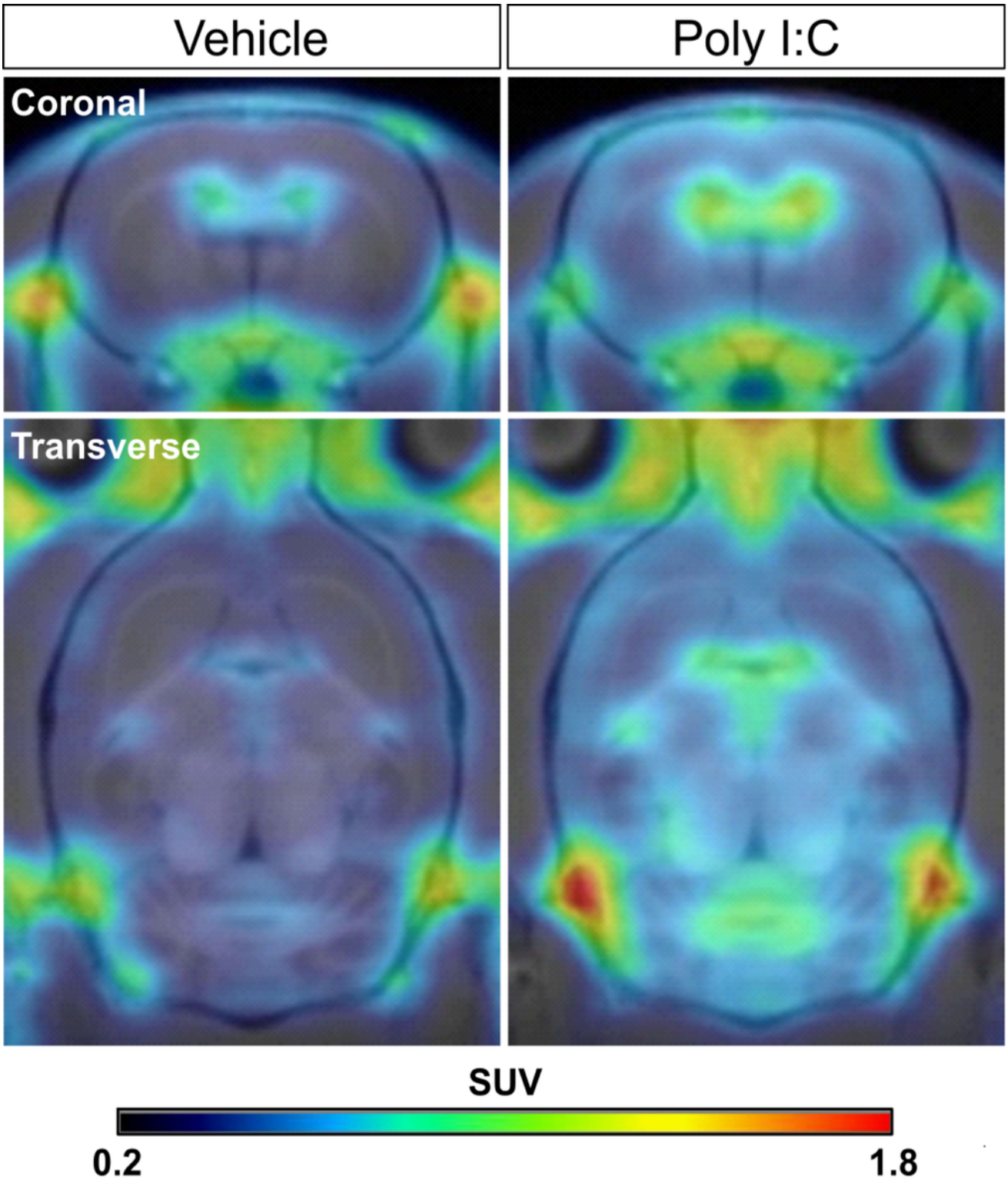

Figure 3

Representative [^{18}F]DPA-714 PET images co-registered with an MRI template in the control and poly I:C-treated rats.

The coronal and transverse views of representative PET images were shown. PET scan with [^{18}F]DPA-714 was performed in rats from both groups at 24 h after poly I:C or vehicle injection. PET images were

reconstructed with a MAP algorithm and summed from 5 to 45 min following a [^{18}F]DPA-714 bolus injection.

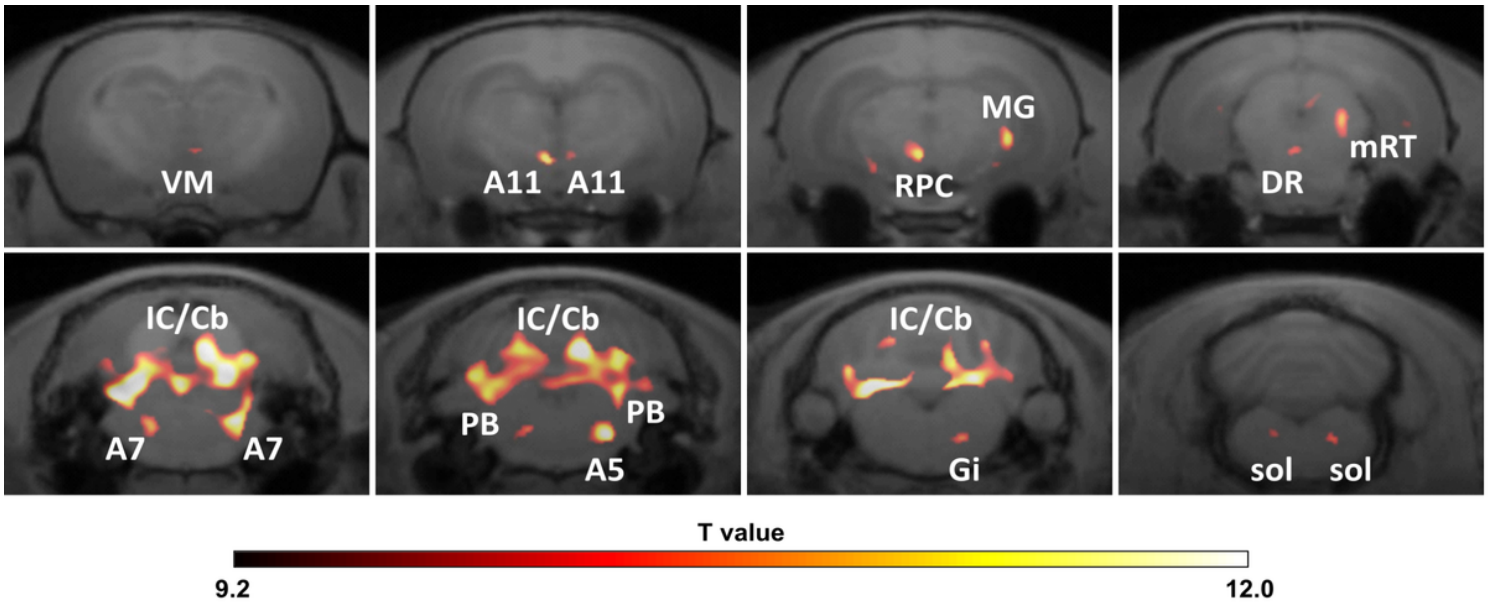

Figure 4

Significant increment of regional neuroinflammation following peripheral pseudoinfection.

Images were obtained by voxel-based statistical comparison of [^{18}F]DPA-714 accumulation in entire brain regions between vehicle (n = 8) and poly I:C (n = 8) injected rats and co-registered with an MRI template. The T value of 9.14 was used as the threshold corresponding to the P < 0.005 (FWE) threshold. The right side of images corresponds to the right hemisphere. VM, ventromedial thalamic nucleus; A11, A11 region; RPC, parvicellular part of red nucleus; MG, medial geniculate nucleus; DR, dorsal raphe nucleus; mRT, mesencephalic reticular formation; A7, A7 noradrenergic nucleus; IC/Cb, inferior colliculus/cerebellum; PB, parabrachial nucleus; A5, A5 noradrenergic nucleus; Gi, gigantocellular reticular nucleus; sol, nucleus tractus solitarius.

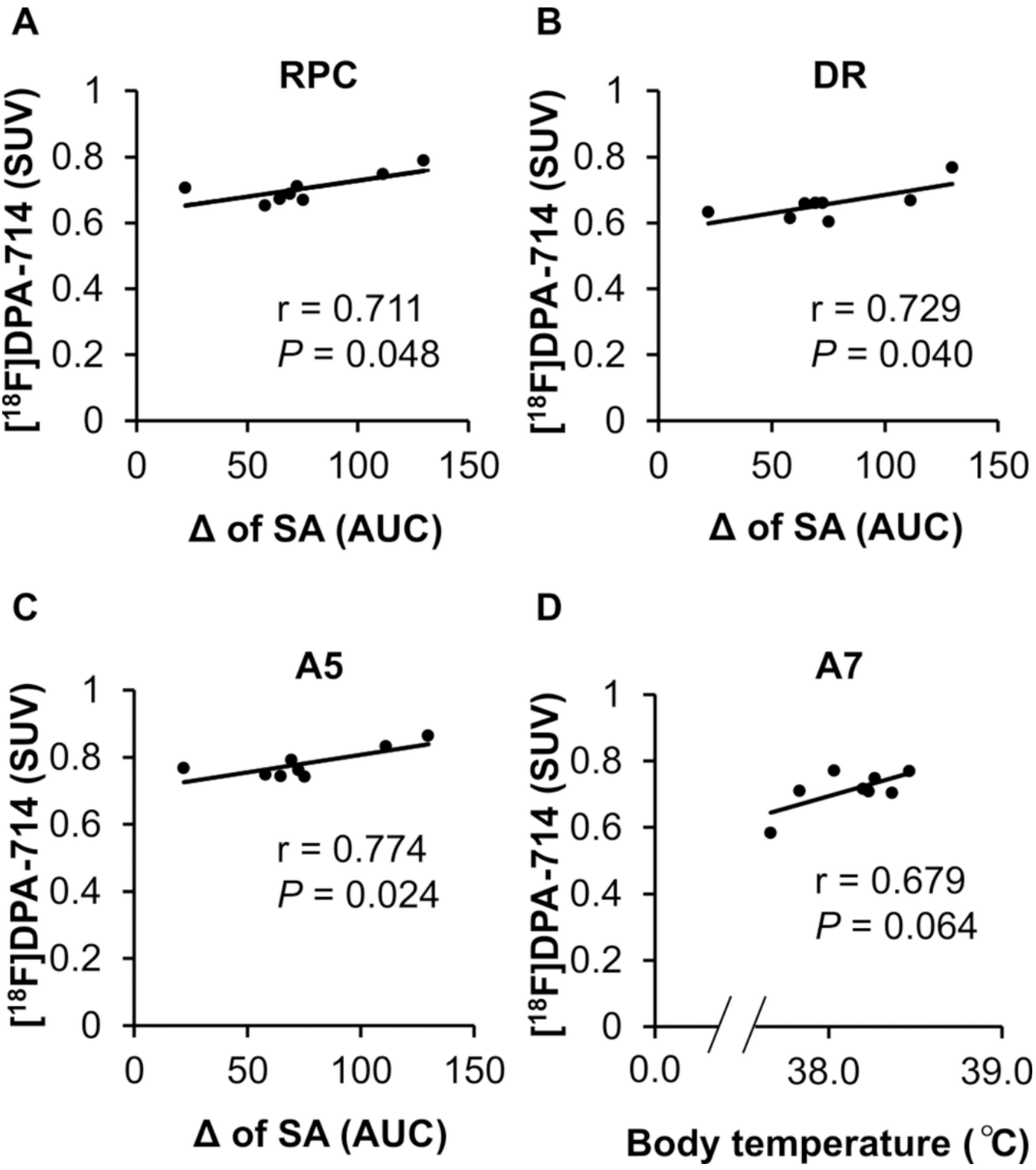

Figure 5

Correlation between regional neuroinflammation in brain areas and fatigue-like behavior.

(A, B, and C) The correlation between neuroinflammation in the RPC, DR and A5 and night-time spontaneous activity. The positive correlation between the accumulation of [^{18}F]DPA-714 in the RPC, DR, and A5 at 24 h after poly I:C injection with a prolonged decrease in night-time spontaneous activity from

day 2 to day 5 following poly I:C injection. The Pearson coefficient value (r) is shown for each relation. RPC, parvicellular part of red nucleus; DR, dorsal raphe nucleus; A5, A5 noradrenergic nucleus; SA, night-time spontaneous activity. **(D)** The correlation between neuroinflammation in the A7 and body temperature. The tendency towards a positive correlation between the accumulation of [^{18}F]DPA-714 in the A7 at 24 h following poly I:C injection and an elevated body temperature following poly I:C injection. The Pearson coefficient value (r) is shown for the relation. A7, A7 noradrenergic nucleus.